PERGAMON

International Journal of Solids and Structures 40 (2003) 1943–1958

INTERNATIONAL JOURNAL OF SOLIDS and STRUCTURES

www.elsevier.com/locate/ijsolstr

Arbitrarily oriented crack near interface in piezoelectric bimaterials

Wen-ye Tian *, K.T. Chau

Department of Civil and Structural Engineering, Hong Kong Polytechnic University, Hung Hom, Kowloon, Hong Kong

Received 1 April 2002; received in revised form 20 August 2002

Abstract

Arbitrarily oriented crack near interface in piezoelectric bimaterials is considered. After deriving the fundamental solution for an edge dislocation near the interface, the present problem can be expressed as a system of singular integral equations by modeling the crack as continuously distributed edge dislocations. In the paper, the dislocations are described by a density function defined on the crack line. By solving the singular integral equations numerically, the dislocation density function is determined. Then, the stress intensity factors (SIFs) and the electric displacement intensity factor (EDIF) at the crack tips are evaluated. Subsequently, the influences of the interface on crack tip SIFs, EDIF, and the mechanical strain energy release rate (MSERR) are investigated. The J-integral analysis in piezoelectric bimaterals is also performed. It is found that the path-independent of J_1-integral and the path-dependent of J_2-integral found in no-piezoelectric bimaterials are still valid in piezoelectric bimaterials.

Keywords: Piezoelectric bimaterials; Interface; Crack; Dislocation; J-integral

1. Introduction

With the extensive use of piezoelectric materials in smart devices such as sensors and actuators, the cracking problems in such kind of materials have drawn increasing attention recently. As today, the behaviors of crack in homogeneous piezoelectrics subjected to combined mechanical and electric loads have been studied sufficiently (see Deeg, 1980; McMeeking, 1990; Pak, 1990, 1992; Sosa and Pak, 1990; Sosa, 1991, 1992; Park and Sun, 1995a,b; Han and Chen, 1999). For example, Sosa (1992) reported that, for one single crack in homogeneous piezoelectric ceramics, the stress intensity factors (SIFs) are independent of the remote electric loading and the electric displacement intensity factor (EDIF) is independent of the remote mechanical loading. With the aid of the total energy release rate, Pak (1992) found that an electric field generally impeded the growth of crack. To describe the stability of a typical crack in homogeneous piezoelectric ceramics, Park and Sun (1995a,b) further proposed a new fracture parameter, namely the

* Corresponding author.
E-mail address: Tianwenye@hotmail.com (W.-y. Tian).

0020-7683/02/$ - see front matter © 2002 Published by Elsevier Science Ltd.
doi:10.1016/S0020-7683(02)00493-6

mechanical strain energy release rate (MSERR). On the study of the similar problems in dissimilar piezoelectric materials, Suo et al. (1992) studied interface crack problems and derived the fundamental solution of the interface crack. Soh et al. (2000) analyzed the behavior of a bi-piezoelectric ceramic layer with interfacial crack subjected to anti-plane shear and in-plane electric loading, moreover investigated the effects of the layer thickness and the material constants of the two dissimilar materials on the fracture behavior. But in comparison, the fracture behaviors of arbitrarily oriented crack near interface in piezoelectric bimaterials have not been studied sufficiently.

Due to the dislocation method provides simplifications in formulation and solution, it has been successfully applied to solve many crack problems in both elastic media (see e.g., He and Hutchinson, 1989; Lu and Lardner, 1992; Suo and Hutchinson, 1989; Miller, 1989) and piezoelectric media (see e.g., Barnett and Lothe, 1975; Pak, 1992; Gao et al., 1997; Fulton and Gao, 1997; Qin and Mai, 2000; Soh et al., 2000). For elastic media, the continuously distributed dislocation described by a density function is used only to model the crack. However, for piezoelectric media, not only the crack need to be modeled by the continuously distributed dislocation, but also the electric potential jump across the crack is required to be simulated by the distribution of electric potential dislocations. Following this idea, Barnett and Lothe (1975) generalized the Stroh formalism to include the electric potential jump across the slip plane in piezoelectric materials. Pak (1992) investigated the electroelastic fields and the energy release rate for a finite crack by modeling a crack as the distributed dislocations and electric dipoles. Gao et al. (1997) and Fulton and Gao (1997) investigated the effect of an electric polarization saturation strip confined in a line segment in front of a crack. Qin and Mai (2000) studied the crack branch problems in piezoelectric bimaterial solid. However, little effort has been made to apply this method to analyze the near interface crack problems in piezoelectric bimaterials.

In view of above reasons, the arbitrarily oriented crack near the interface of piezoelectric bimaterials will be studied in this paper by using the edge dislocation method. The paper is organized as follows. In Section 2, a fundamental solution for an edge dislocation near the interface of a piezoelectric bimaterial is derived. In Section 3, the present crack problem is reduced to a system of singular integral equations by modeling the crack using continuously distributed dislocations. In Section 4, the crack tips SIFs and EDIF as well as MSERR are evaluated. In Section 5, the J-integral analysis is performed. In Section 6, numerical results derived under several remote loading conditions are given.

2. Formula and solutions

2.1. Fundamental theory

It is well known that the strain γ and the electric field E in piezoelectric material could be derived from the gradients of the displacement u and the electric potential ϕ

$$\gamma_{ij} = \tfrac{1}{2}\left(u_{i,j} + u_{j,i}\right), \quad E_i = -\phi_{,i} \qquad (i,j = 1,2,3) \tag{1}$$

and the stress σ_{ij} and the electric displacement D_i are related by following constitutive relations:

$$\sigma_{ij} = C_{ijrs}\gamma_{rs} - e_{sji}E_s, \quad D_i = \varepsilon_{is}E_s + e_{irs}\gamma_{rs} \qquad (i,j,r,s = 1,2,3) \tag{2}$$

where C_{ijrs} represents the elastic stiffness constants, e_{sji} the piezoelectric constants and ε_{is} the dielectric constants, respectively.

Suo et al. (1992) has found that, for a two-dimensional problem, i.e., with geometry and external loading invariant in the direction normal to xy-plane, the elastic field and the electric field could be represented in terms of four complex functions $f_1(z_1)$, $f_2(z_2)$, $f_3(z_3)$, and $f_4(z_4)$, each of which is holomorphic in its argument $z_j = x + \mu_j y$ $(j = 1,2,3,4)$. Here μ_j are four distinct complex numbers with positive imaginary

parts. With these holomorphic functions (or complex potentials), the general solutions for steady-state plane piezoelectricity could be represented as

$$\begin{aligned}
\{u_i\} &= 2\mathrm{Re}\sum_{j=1}^{4} A_{ij} f_j(z_j), \\
\{\sigma_{2i}\} &= 2\mathrm{Re}\sum_{j=1}^{4} L_{ij} f_j'(z_j), \quad i = 1,2,3,4 \\
\{\sigma_{1i}\} &= -2\mathrm{Re}\sum_{j=1}^{4} L_{ij}\mu_j f_j'(z_j)
\end{aligned} \tag{3}$$

where $\{u_i\} = \{u_1, u_2, u_3, \phi\}$, $\{\sigma_{1i}\} = \{\sigma_{11}, \sigma_{12,}\sigma_{13}, D_1\}$, $\{\sigma_{2i}\} = \{\sigma_{21}, \sigma_{22,}\sigma_{23}, D_2\}$. u_i ($i = 1, 2, 3$) represents the displacements, u_4 (i.e., ϕ) the electric potential, σ_{ij} the stress, and D the electric displacement. A_{ij} and L_{ij} are matrices depending on material constants (Suo et al., 1992).

Introduce a vector function (Suo, 1990)

$$f'(z) = [f_1'(z), f_2'(z), f_3'(z), f_4'(z)]^{\mathrm{T}} \tag{4}$$

where $z = x + \mu y$ ($\mathrm{Im}\,\mu > 0$). Once the solution of $f'(z)$ is obtained for a given boundary value problem, the variable z should be replaced with the argument z_j when calculating field quantities from (3).

2.2. Dislocation

Consider an infinite piezoelectric bimaterial plate with materials 1 and 2 occupying the upper and lower half planes, respectively. Assume there exists a near-interface dislocation singularity in material 2, the (x, y) is the Cartesian global coordinate system (see Fig. 1).

Following the procedure of Miller (1989) for dissimilar anisotropic elasticity, the general dislocation solution to the piezoelectric bimaterial problem will be derived in this section. Define a new set of potentials Ψ_k in terms of f_j' for the lower half plane and $f_j'^*$ for the upper half plane such that for the lower half plane $\mathrm{Im}\{z\} < 0$

$$\begin{bmatrix} \Psi_1(z) \\ \Psi_2(z) \\ \Psi_3(z) \\ \Psi_4(z) \\ \Psi_5(z) \\ \Psi_6(z) \\ \Psi_7(z) \\ \Psi_8(z) \end{bmatrix} = \begin{bmatrix} A_{11} & A_{12} & A_{13} & A_{14} & -\overline{A_{11}^*} & -\overline{A_{12}^*} & -\overline{A_{13}^*} & -\overline{A_{14}^*} \\ A_{21} & A_{22} & A_{23} & A_{24} & -\overline{A_{21}^*} & -\overline{A_{22}^*} & -\overline{A_{23}^*} & -\overline{A_{24}^*} \\ A_{31} & A_{32} & A_{33} & A_{34} & -\overline{A_{31}^*} & -\overline{A_{32}^*} & -\overline{A_{33}^*} & -\overline{A_{34}^*} \\ A_{41} & A_{42} & A_{43} & A_{44} & -\overline{A_{41}^*} & -\overline{A_{42}^*} & -\overline{A_{43}^*} & -\overline{A_{44}^*} \\ L_{11} & L_{12} & L_{13} & L_{14} & -\overline{L_{11}^*} & -\overline{L_{12}^*} & -\overline{L_{13}^*} & -\overline{L_{14}^*} \\ L_{21} & L_{22} & L_{23} & L_{24} & -\overline{L_{21}^*} & -\overline{L_{22}^*} & -\overline{L_{23}^*} & -\overline{L_{24}^*} \\ L_{31} & L_{32} & L_{33} & L_{34} & -\overline{L_{31}^*} & -\overline{L_{32}^*} & -\overline{L_{33}^*} & -\overline{L_{34}^*} \\ L_{41} & L_{42} & L_{43} & L_{44} & -\overline{L_{41}^*} & -\overline{L_{42}^*} & -\overline{L_{43}^*} & -\overline{L_{44}^*} \end{bmatrix} \begin{bmatrix} f_1'(z) \\ f_2'(z) \\ f_3'(z) \\ f_4'(z) \\ \overline{f_1'^*}(z) \\ \overline{f_2'^*}(z) \\ \overline{f_3'^*}(z) \\ \overline{f_4'^*}(z) \end{bmatrix} \tag{5}$$

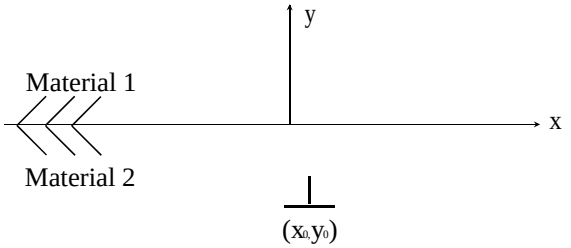

Fig. 1. Edge dislocation near the interface.

for the upper half plane $\mathrm{Im}\{z\} > 0$

$$\begin{bmatrix} \Psi_1(z) \\ \Psi_2(z) \\ \Psi_3(z) \\ \Psi_4(z) \\ \Psi_5(z) \\ \Psi_6(z) \\ \Psi_7(z) \\ \Psi_8(z) \end{bmatrix} = \begin{bmatrix} A_{11}^* & A_{12}^* & A_{13}^* & A_{14}^* & -\overline{A_{11}} & -\overline{A_{12}} & -\overline{A_{13}} & -\overline{A_{14}} \\ A_{21}^* & A_{22}^* & A_{23}^* & A_{24}^* & -\overline{A_{21}} & -\overline{A_{22}} & -\overline{A_{23}} & -\overline{A_{24}} \\ A_{31}^* & A_{32}^* & A_{33}^* & A_{34}^* & -\overline{A_{31}} & -\overline{A_{32}} & -\overline{A_{33}} & -\overline{A_{34}} \\ A_{41}^* & A_{42}^* & A_{43}^* & A_{44}^* & -\overline{A_{41}} & -\overline{A_{42}} & -\overline{A_{43}} & -\overline{A_{44}} \\ L_{11}^* & L_{12}^* & L_{13}^* & L_{14}^* & -\overline{L_{11}} & -\overline{L_{12}} & -\overline{L_{13}} & -\overline{L_{14}} \\ L_{21}^* & L_{22}^* & L_{23}^* & L_{24}^* & -\overline{L_{21}} & -\overline{L_{22}} & -\overline{L_{23}} & -\overline{L_{24}} \\ L_{31}^* & L_{32}^* & L_{33}^* & L_{34}^* & -\overline{L_{31}} & -\overline{L_{32}} & -\overline{L_{33}} & -\overline{L_{34}} \\ L_{41}^* & L_{42}^* & L_{43}^* & L_{44}^* & -\overline{L_{41}} & -\overline{L_{42}} & -\overline{L_{43}} & -\overline{L_{44}} \end{bmatrix} \begin{bmatrix} f_1'^*(z) \\ f_2'^*(z) \\ f_3'^*(z) \\ f_4'^*(z) \\ \overline{f_1'}(z) \\ \overline{f_2'}(z) \\ \overline{f_3'}(z) \\ \overline{f_4'}(z) \end{bmatrix} \tag{6}$$

Here and throughout the paper, superscript '$*$' indicates the upper half plane. In Eqs. (5) and (6), the overbar denotes complex conjugation. Now, the jump in each of the physical quantities (σ_{2j}, u_j $(j = 1, 2, 3)$, D_2 and ϕ) across the interface is given by $\Psi_k^+(x) - \Psi_k^-(x)$ $(k = 1, 2, \ldots, 8)$.

To model dislocation, the following complex potentials corresponding to the basic singular solution for plane piezoelectric body are considered:

$$f_j'(z) = \frac{B_j}{z - z_{0j}} \tag{7}$$

in which $z_{0j} = x_0 + \mu_j y_0$, with x_0 and y_0 locating the singularity. The B_j are complex constants related to the net force, displacement, electric displacement and electric potential jump induced by the singularity as follows:

$$\begin{aligned} \mathrm{Im} \sum_{j=1}^{4} L_{ij} B_j &= -\frac{X_i}{4\pi} \\ \mathrm{Im} \sum_{j=1}^{4} A_{ij} B_j &= -\frac{\Delta u_i}{4\pi} \end{aligned} \qquad (i = 1, 2, 3, 4) \tag{8}$$

The quantities X_1 and X_2 represent the x and y components of the net force, $X_3 = 0$, and X_4 the net electric displacement on any contour encircling the singularity, and Δu_1, Δu_2 and Δu_3 the displacement jumps in the u_1, u_2 and u_3 displacements and Δu_4 the electric potential jump in the ϕ electric potential. For the case of a pure dislocation singularity, X_i $(i = 1, 2, 3, 4)$ are taken to be zero.

Then, substitute Eq. (7) into Eqs. (5) and (6), the potentials Ψ corresponding to the f_j' of Eq. (7) can be calculated directly. Provided the singularity locate in the lower half plane and $f_j'^* = 0$, then

for the lower half plane $\mathrm{Im}\{z\} < 0$

$$\Psi_k(z) = \sum_{j=1}^{4} C_{kj} \frac{B_j}{z - z_{0j}} \tag{9}$$

for the upper half plane $\mathrm{Im}\{z\} > 0$

$$\Psi_k(z) = \sum_{j=1}^{4} -\overline{C}_{kj} \frac{\overline{B}_j}{z - \bar{z}_{0j}} \tag{10}$$

where

$$\begin{aligned} C_{kj} &= A_{kj} \\ C_{(k+4)j} &= L_{kj} \end{aligned} \qquad (k, j = 1, 2, 3, 4) \tag{11}$$

From Eqs. (9) and (10), it is easily found that $\Psi_k^+(x) - \Psi_k^-(x) \neq 0$, in other words, the interface condition is not satisfied, the traction, electric displacement, displacements and electric potential are not continuous across the interface. To satisfy the interface condition, the following additional potentials are introduced

$$\widehat{\Psi}_k(z) = \begin{cases} \sum_{j=1}^{4} -\overline{C}_{kj} \dfrac{\overline{B}_j}{z - \bar{z}_{0j}} & \mathrm{Im}\{z\} < 0 \\ \sum_{j=1}^{4} C_{kj} \dfrac{B_j}{z - z_{0j}} & \mathrm{Im}\{z\} > 0 \end{cases} \tag{12}$$

Add Eqs. (9), (10) and (12) together, the sum Ψ_k becomes

$$\Psi_k(z) = \sum_{j=1}^{4} \left\{ C_{kj} \frac{B_j}{z - z_{0j}} - \overline{C}_{kj} \frac{\overline{B}_j}{z - \bar{z}_{0j}} \right\} \tag{13}$$

Obviously, Eq. (13) has satisfied the interface condition.

Using the relations (5) and (6), the complex potentials f_j' can be expressed in term of the Ψ_j as follows:

for the lower half plane $\mathrm{Im}\{z\} < 0$

$$\begin{aligned} f_j'(z) &= m_{jk} \Psi_k(z) \\ \overline{f_j'(z)} &= -\overline{m_{jk}} \Psi_k(\bar{z}) \end{aligned} \quad (j,k = 1,2,3,4) \tag{14}$$

for the upper half plane $\mathrm{Im}\{z\} > 0$

$$\begin{aligned} f_j'^*(z) &= -\overline{m_{(j+4)k}} \Psi_k(z) \\ \overline{f_j'^*(z)} &= m_{(j+4)k} \Psi_k(\bar{z}) \end{aligned} \quad (j,k = 1,2,3,4) \tag{15}$$

where m_{jk} are the components of the inverse of the matrix in Eq. (5).

Thus the potentials f_j' modeling a dislocation singularity near piezoelectric bimaterial interface are as follows:

$$f_j'(z) = \frac{B_j}{z - z_{0j}} - \sum_{k=1}^{8} m_{jk} \sum_{i=1}^{4} \overline{C}_{ki} \frac{\overline{B}_i}{z - \bar{z}_{0i}} \tag{16}$$

Now, using Eqs. (3) and (16), the stress field and electric field due to the edge dislocation at near interface point z_0 can be evaluated without any difficulty

$$\begin{aligned} \{\sigma_{2i}\} &= 2\mathrm{Re} \sum_{j=1}^{4} L_{ij} \left[\frac{B_j}{z - z_{0j}} - \sum_{k=1}^{8} m_{jk} \sum_{i=1}^{4} \overline{C}_{ki} \frac{\overline{B}_i}{z - \bar{z}_{0i}} \right], \\ \{\sigma_{1i}\} &= -2\mathrm{Re} \sum_{j=1}^{4} L_{ij} \mu_j \left[\frac{B_j}{z - z_{0j}} - \sum_{k=1}^{8} m_{jk} \sum_{i=1}^{4} \overline{C}_{ki} \frac{\overline{B}_i}{z - \bar{z}_{0i}} \right] \end{aligned} \tag{17}$$

where $\{\sigma_{1i}\} = \{\sigma_{11}, \sigma_{12,}\sigma_{13}, D_1\}$, $\{\sigma_{2i}\} = \{\sigma_{21}, \sigma_{22,}\sigma_{23}, D_2\}$.

3. Singular integral equation

Consider an infinite piezoelectric bimaterial plate containing a near interface crack AB with orientation angle β and length l as shown in Fig. 2. l' is the distance between the crack tip A and intersection point of the crack line and the interface. The crack is simulated by continuous distributed dislocations. The electric elastic field arising from the distributed dislocations and that arising from an applied loading should satisfy the traction-free and charge-free on crack faces. Let $B_j(\xi)(0 < \xi < l)$ $(j = 1,2,3,4)$ denotes the densities of distributed dislocations along the crack line. Using the fundamental solution derived above, the following singular integral equations are deduced

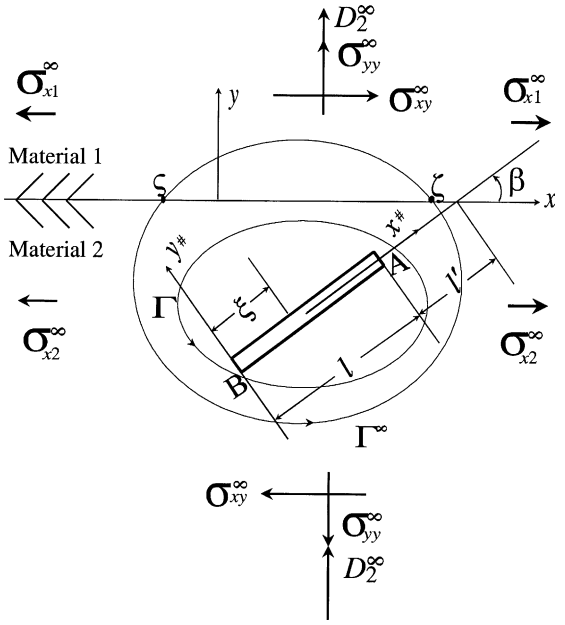

Fig. 2. A crack with two closed contours.

$$
\begin{aligned}
&2\mathrm{Re}\sum_{j=1}^{4}\left\{\begin{array}{l}(-L_{1j}\mu_j\sin^2\beta+L_{2j}\cos^2\beta-L_{1j}\sin 2\beta)\left[\displaystyle\int_0^l\frac{B_j(\xi)\,\mathrm{d}\xi}{(\eta-\xi)(\cos\beta+\mu_j\sin\beta)}\right.\\ \left.-\displaystyle\sum_{k=1}^{8}m_{jk}\sum_{i=1}^{4}\overline{C}_{ki}\int_0^l\frac{\overline{B}_i(\xi)\,\mathrm{d}\xi}{(\mu_j-\overline{\mu}_i)y_0+(\eta-\xi)\cos\beta+(\eta\mu_j-\xi\overline{\mu}_i)\sin\beta}\right]\end{array}\right\}=p(\eta)\\
&2\mathrm{Re}\sum_{j=1}^{4}\left\{\begin{array}{l}(L_{1j}\mu_j\sin\beta\cos\beta+L_{2j}\sin\beta\cos\beta+L_{1j}\cos 2\beta)\left[\displaystyle\int_0^l\frac{B_j(\xi)\,\mathrm{d}\xi}{(\eta-\xi)(\cos\beta+\mu_j\sin\beta)}\right.\\ \left.-\displaystyle\sum_{k=1}^{8}m_{jk}\sum_{i=1}^{4}\overline{C}_{ki}\int_0^l\frac{\overline{B}_i(\xi)\,\mathrm{d}\xi}{(\mu_j-\overline{\mu}_i)y_0+(\eta-\xi)\cos\beta+(\eta\mu_j-\xi\overline{\mu}_i)\sin\beta}\right]\end{array}\right\}=q(\eta)\\
&2\mathrm{Re}\sum_{j=1}^{4}\left\{\begin{array}{l}(L_{3j}\mu_j\sin\beta+L_{3j}\cos\beta)\left[\displaystyle\int_0^l\frac{B_j(\xi)\,\mathrm{d}\xi}{(\eta-\xi)(\cos\beta+\mu_j\sin\beta)}\right.\\ \left.-\displaystyle\sum_{k=1}^{8}m_{jk}\sum_{i=1}^{4}\overline{C}_{ki}\int_0^l\frac{\overline{B}_i(\xi)\,\mathrm{d}\xi}{(\mu_j-\overline{\mu}_i)y_0+(\eta-\xi)\cos\beta+(\eta\mu_j-\xi\overline{\mu}_i)\sin\beta}\right]\end{array}\right\}=r(\eta)\\
&2\mathrm{Re}\sum_{j=1}^{4}\left\{\begin{array}{l}(L_{4j}\mu_j\sin\beta+L_{4j}\cos\beta)\left[\displaystyle\int_0^l\frac{B_j(\xi)\,\mathrm{d}\xi}{(\eta-\xi)(\cos\beta+\mu_j\sin\beta)}\right.\\ \left.-\displaystyle\sum_{k=1}^{8}m_{jk}\sum_{i=1}^{4}\overline{C}_{ki}\int_0^l\frac{\overline{B}_i(\xi)\,\mathrm{d}\xi}{(\mu_j-\overline{\mu}_i)y_0+(\eta-\xi)\cos\beta+(\eta\mu_j-\xi\overline{\mu}_i)\sin\beta}\right]\end{array}\right\}=d(\eta)
\end{aligned}
\tag{18}
$$

where the functions $p(\eta)$, $q(\eta)$, $r(\eta)$ are the known tractions and $d(\eta)$ the electric displacement due to the applied loading.

In addition, we have the condition

$$\int_0^l B_j(\xi)\,\mathrm{d}\xi = 0 \tag{19}$$

Then integral equation (18) can be solved numerically using the method developed by Erdogan (1978), the functions $B_j(\xi)$ are replaced with square root singular expressions as follows:

$$B_j(\xi) = \frac{B_{0j}(\xi)}{\sqrt{\xi(l-\xi)}} \tag{20}$$

where $B_{0j}(\xi)$ are the non-singular part of $B_j(\xi)$.

4. Crack tip parameters

The SIFs and the EDIF at the crack tip $\xi = l$ are

$$\begin{aligned}
K_{\mathrm{I}} &= \frac{(2\pi)^{3/2}}{\sqrt{l}}\,\mathrm{Re}\sum_{j=1}^{4}\left\{\left(-L_{1j}\mu_j\sin^2\beta + L_{2j}\cos^2\beta - L_{1j}\sin 2\beta\right)\frac{B_{0j}(l)}{(\cos\beta+\mu_j\sin\beta)}\right\}\\
K_{\mathrm{II}} &= \frac{(2\pi)^{3/2}}{\sqrt{l}}\,\mathrm{Re}\sum_{j=1}^{4}\left\{\left(L_{1j}\mu_j\sin\beta\cos\beta + L_{2j}\sin\beta\cos\beta + L_{1j}\cos 2\beta\right)\frac{B_{0j}(l)}{(\cos\beta+\mu_j\sin\beta)}\right\}\\
K_{\mathrm{III}} &= \frac{(2\pi)^{3/2}}{\sqrt{l}}\,\mathrm{Re}\sum_{j=1}^{4}\left\{\left(L_{3j}\mu_j\sin\beta + L_{3j}\cos\beta\right)\frac{B_{0j}(l)}{(\cos\beta+\mu_j\sin\beta)}\right\}\\
K_{\mathrm{e}} &= \frac{(2\pi)^{3/2}}{\sqrt{l}}\,\mathrm{Re}\sum_{j=1}^{4}\left\{\left(L_{4j}\mu_j\sin\beta + L_{4j}\cos\beta\right)\frac{B_{0j}(l)}{(\cos\beta+\mu_j\sin\beta)}\right\}
\end{aligned} \tag{21}$$

with an analogous expression at the other tip. Where the subscripts I, II and III refer to the three modes of traditional SIFs, the subscripts e denotes the EDIF.

The MSERR is

$$G_{\mathrm{I}}^{\mathrm{M}} = \lim_{\delta\to 0}\frac{1}{2\delta}\int_0^{\delta}\sigma_{22}(x)\Delta u_2(\delta-x)\,\mathrm{d}x \quad \text{for the mode I} \tag{22}$$

and

$$G_{\mathrm{II}}^{\mathrm{M}} = \lim_{\delta\to 0}\frac{1}{2\delta}\int_0^{\delta}\sigma_{12}(x)\Delta u_1(\delta-x)\,\mathrm{d}x \quad \text{for the mode II} \tag{23}$$

where the superscript M refers to the MSERR (Park and Sun, 1995a,b), Δu_1 and Δu_2 are the jumps of the displacement components measured from the lower face to the upper face of the crack.

For the modes I and II, the MSERR are related with the crack tip SIFs and EDIF as follows:

$$G_{\mathrm{I}}^{\mathrm{M}} = \tfrac{1}{4}(H_{21}K_{\mathrm{I}}K_{\mathrm{II}} + H_{22}(K_{\mathrm{I}})^2 + H_{23}K_{\mathrm{I}}K_{\mathrm{III}} + H_{24}K_{\mathrm{I}}K_{\mathrm{e}}) \tag{24}$$

and

$$G_{\mathrm{II}}^{\mathrm{M}} = \tfrac{1}{4}(H_{11}(K_{\mathrm{II}})^2 + H_{12}K_{\mathrm{I}}K_{\mathrm{II}} + H_{13}K_{\mathrm{II}}K_{\mathrm{III}} + H_{14}K_{\mathrm{II}}K_{\mathrm{e}}) \tag{25}$$

where H_{ij} (i, $j = 1, 2, 3, 4$) is the elements of the following 4×4 matrix $\mathbf{H}$

$$\mathbf{H} = \mathrm{i}\mathbf{A}\mathbf{L}^{-1} + \overline{\mathrm{i}\mathbf{A}\mathbf{L}^{-1}} \quad (\mathrm{i} = \sqrt{-1}) \tag{26}$$

where $\mathbf{A}$ and $\mathbf{L}$ are for the lower half plane material.

5. *J*-integral analysis

Consider a near interface crack with oriented angle β and the applied remote stresses and electric displacement σ_{yy}^{∞}, σ_{xy}^{∞}, σ_{x1}^{∞}, σ_{x2}^{∞}, D_2^{∞} as shown in Fig. 2. In order to perform the J-integral analysis, two kinds of closed contours Γ^{∞} and Γ are introduced. Here, the global system (x, y) is attached to the interface, while the local coordinate system $(x^{\#}, y^{\#})$ is attached to the crack oriented by an angle β with respect to the x-axis or the interface. It should be emphasized that Γ^{∞} encloses the crack completely and cuts the interface at points ς and ζ, Γ only encloses the crack completely and does not cut the interface. For the contour Γ, the J-integral in the global coordinate system (x, y) is as follows (Pak, 1990; Suo et al., 1992):

$$J = J_1 = \oint_{\Gamma} \left\{ \frac{1}{2}(\sigma_{ij}\gamma_{ij} - D_i E_i)\,\mathrm{d}y - n_i \sigma_{ip} \frac{\partial u_p}{\partial x}\,\mathrm{d}s - n_i D_i \frac{\partial \phi}{\partial x}\,\mathrm{d}s \right\} \quad (i, j, p = 1, 2) \tag{27}$$

where n_i is the outer normal to the contour Γ.

Similarly, the formulation for the second component of the J_k-vector (Budiansky and Rice, 1973) in piezoelectric materials is

$$J_2 = \oint_{\Gamma} \left\{ -\frac{1}{2}(\sigma_{ij}\gamma_{ij} - D_i E_i)\,\mathrm{d}x - n_i \sigma_{ip} \frac{\partial u_p}{\partial y}\,\mathrm{d}s - n_i D_i \frac{\partial \phi}{\partial y}\,\mathrm{d}s \right\} \tag{28}$$

It should be emphasized that the J_2-integral, as discussed by Herrmann and Herrmann (1981), is generally path-dependent. However, in the undermentioned manipulations, it is always assumed that the closed contour Γ chosen to calculate the J_2-integral encloses the crack completely. So under this assumption, the integral is actually path-independent.

In local coordinate system $(x^{\#}, y^{\#})$, the J_1 and J_2 integrals along the contour Γ are

$$J_1^{\#} = \oint_{\Gamma} \left\{ \frac{1}{2}(\sigma_{ij}^{\#}\gamma_{ij}^{\#} - D_i^{\#} E_i^{\#})\,\mathrm{d}y^{\#} - n_i^{\#} \sigma_{ip}^{\#} \frac{\partial u_p^{\#}}{\partial x^{\#}}\,\mathrm{d}s - n_i^{\#} D_i^{\#} \frac{\partial \phi^{\#}}{\partial x^{\#}}\,\mathrm{d}s \right\} \tag{29}$$

$$J_2^{\#} = \oint_{\Gamma} \left\{ -\frac{1}{2}(\sigma_{ij}^{\#}\gamma_{ij}^{\#} - D_i^{\#} E_i^{\#})\,\mathrm{d}x^{\#} - n_i^{\#} \sigma_{ip}^{\#} \frac{\partial u_p^{\#}}{\partial y^{\#}}\,\mathrm{d}s - n_i^{\#} D_i^{\#} \frac{\partial \phi^{\#}}{\partial y^{\#}}\,\mathrm{d}s \right\} \tag{30}$$

where all quantities in Eqs. (29) and (30) are defined in the local coordinate system $(x^{\#}, y^{\#})$, and the subscripts i, j and $p = 1, 2, 3$.

Performing a transformation from system (x, y) to system $(x^{\#}, y^{\#})$, the following formulations could be obtained:

$$\begin{aligned} J_1 &= J_1^{\#} \cos\beta - J_2^{\#} \sin\beta \\ J_2 &= J_1^{\#} \sin\beta + J_2^{\#} \cos\beta \end{aligned} \tag{31}$$

In above equations, $J_1^{\#}$ and $J_2^{\#}$ can be expressed in the following form (Suo et al., 1992):

$$J_1^{\#} = \frac{1}{4}(\mathbf{K}^{\mathrm{R}})^{\mathrm{T}}\mathbf{H}\mathbf{K}^{\mathrm{R}} - \frac{1}{4}(\mathbf{K}^{\mathrm{L}})^{\mathrm{T}}\mathbf{H}\mathbf{K}^{\mathrm{L}} \tag{32}$$

$$J_2^{\#} = \frac{1}{4}(\mathbf{K}^{\mathrm{R}})^{\mathrm{T}}\mathbf{X}\mathbf{H}\mathbf{K}^{\mathrm{R}} - \frac{1}{4}(\mathbf{K}^{\mathrm{L}})^{\mathrm{T}}\mathbf{X}\mathbf{H}\mathbf{K}^{\mathrm{L}} + \int_0^l (W^+ - W^-)\,\mathrm{d}x^{\#} \tag{33}$$

where

$$\begin{aligned}\mathbf{K}^{\mathrm{R}} &= [K_{\mathrm{II}}^{\mathrm{R}}; K_{\mathrm{I}}^{\mathrm{R}}; K_{\mathrm{III}}^{\mathrm{R}}; K_{\mathrm{e}}^{\mathrm{R}}]\\ \mathbf{K}^{\mathrm{L}} &= [K_{\mathrm{II}}^{\mathrm{L}}; K_{\mathrm{I}}^{\mathrm{L}}; K_{\mathrm{III}}^{\mathrm{L}}; K_{\mathrm{e}}^{\mathrm{L}}]\end{aligned} \tag{34}$$

$$\mathbf{X} = -\mathrm{Re}(\mathbf{G}\mathbf{L}^{-1}) \tag{35}$$

$$G_{ij} = L_{ij}\mu_j \quad (i,j = 1,2,3,4) \tag{36}$$

where R and L represent the right and left crack tips, W^+ and W^- in Eq. (33) denote the boundary values of the mechanical and electric energy density W on the upper and lower faces, respectively.

Moreover, as shown in Fig. 2, a confusion may be concerned when using the contour Γ^{∞} instead of Γ in the coordinate system (x, y) since the segment $\varsigma\zeta$ (see Fig. 2) may induce some contribution to the integrals (see Zhao and Chen, 1997). The following manipulations are quite necessary to clarify the confusion:

$$\begin{aligned}J_1^{\infty} &= \oint_{\Gamma^{\infty}} \left\{ \frac{1}{2}(\sigma_{ij}\gamma_{ij} - D_iE_i)\,\mathrm{d}y - n_i\sigma_{ip}\frac{\partial u_p}{\partial x}\,\mathrm{d}s - n_iD_i\frac{\partial \phi}{\partial x}\,\mathrm{d}s \right\}\\ &= \oint_{\Gamma} \left\{ \frac{1}{2}(\sigma_{ij}\gamma_{ij} - D_iE_i)\,\mathrm{d}y - n_i\sigma_{ip}\frac{\partial u_p}{\partial x}\,\mathrm{d}s - n_iD_i\frac{\partial \phi}{\partial x}\,\mathrm{d}s \right.\\ &\quad \left. + \int_{\overline{\varsigma\zeta}} \left[\frac{1}{2}(\sigma_{ij}\gamma_{ij\cdot} - D_iE_i)\right]\mathrm{d}y - n_i\sigma_{ip}\left[\frac{\partial u_p}{\partial x}\right]\mathrm{d}s - n_iD_i\left[\frac{\partial \phi}{\partial x}\right]\mathrm{d}s \right\}\end{aligned} \tag{37}$$

$$\begin{aligned}J_2^{\infty} &= \oint_{\Gamma^{\infty}} \left\{ -\frac{1}{2}(\sigma_{ij}\gamma_{ij} - D_iE_i)\,\mathrm{d}x - n_i\sigma_{ip}\frac{\partial u_p}{\partial y}\,\mathrm{d}s - n_iD_i\frac{\partial \phi}{\partial y}\,\mathrm{d}s \right\}\\ &= \oint_{\Gamma} \left\{ -\frac{1}{2}(\sigma_{ij}\gamma_{ij} - D_iE_i)\,\mathrm{d}x - n_i\sigma_{ip}\frac{\partial u_p}{\partial y}\,\mathrm{d}s - n_iD_i\frac{\partial \phi}{\partial y}\,\mathrm{d}s \right.\\ &\quad \left. + \int_{\overline{\varsigma\zeta}} -\left[\frac{1}{2}\sigma_{ij}\gamma_{ij} - D_iE_i\right]\mathrm{d}x - n_i\sigma_{ip}\left[\frac{\partial u_p}{\partial y}\right]\mathrm{d}s - n_iD_i\left[\frac{\partial \phi}{\partial y}\right]\mathrm{d}s \right\}\end{aligned} \tag{38}$$

where $\overline{\varsigma\zeta}$ in Eqs. (37) and (38) refers to the segment of the interface from ς to ζ point, the bracket [ ] denotes the jump of the corresponding functions across the interface.

Continuous conditions of the displacement, the stresses, the electric displacement, and the electric potential across the interface require that

$$[u_p] = 0, \quad [\sigma_{p2}] = 0, \quad [D_2] = 0 \quad \text{and} \quad [\phi] = 0, \tag{39}$$

which directly lead to the following conclusion as Zhao and Chen (1997) drawn in non-piezoelectric materials:

$$J_1^{\infty} = J_1 \tag{40}$$

Eq. (40) implies that the J_1 integral is path-independent for any contour enclosing the crack in the global coordination system despite of the contour cuts the interface or not. In addition, the applied remote uniform stress field and the applied remote uniform electric field lead to the following conclusion (Zhao and Chen, 1997):

$$J_1^{\infty} = J_1 = 0, \tag{41}$$

due to that there are no other discontinuities outside of the contour.

However, it could be found from Eqs. (38) and (39) that the J_2-integral is path-independent only for a contour enclosing the crack completely but not cutting the interface as Zhao and Chen (1997) concluded in non-piezoelectric bimaterials. Due to the effect induced from the interface, it is not path independent any longer when the integral contour cuts the interface.

6. Numerical results and discussion

Consider a special material combination PZT-5H/PZT-5. Let PZT-5H occupy the upper half-plane, PZT-5 the lower half-plane, respectively. Material constants of the two materials are listed in Table 1. Assume the poling directions of both materials be perpendicular to the interface (the x-axis) (see Fig. 2) and the plane strain condition be satisfied.

First, the accuracy of the proposed numerical scheme is verified by comparing with the numerical results for a near interface crack in an ideal elastic bimaterials. Zhao and Chen (1997) investigated a subinterface crack in bimaterials Cu/Al_2O_3. Consider a fictitious piezoelectric bimaterials with the same elastic constants as Cu/Al_2O_3 identical dielectric constants as PZT-5H in upper half-plane and PZT-5 in lower half-plane, and negligible piezoelectric constants. Here, necessary to note that, a small perturbation of the material constants is employed to obtain distinct eigenvalues in calculation. The remote stress field and the electric field are $\sigma_{yy}^{\infty} = \sigma_{x2}^{\infty} = \sigma$, $\sigma_{xy}^{\infty} = 0$, $\sigma_{x1}^{\infty} \neq 0$ and $D_2^{\infty} = 0$. The ratio of $K_{\mathrm{II}}/K_{\mathrm{I}}$ against the orientation angle β is shown in Fig. 3. Note that these results agree well with those obtained by Zhao and Chen (1997).

In the following, a crack near interface of piezoelectric bimaterials PZT-5H/PZT-5 is investigated. The crack tip SIFs, EDIF and MSERR are evaluated for various geometry and the remote combined mechanical–electric loadings. Necessary to note that, in following calculations, identical mechanical loading is considered, i.e. $\sigma_{yy}^{\infty} = \sigma_{x2}^{\infty} = 4 \times 10^6$ N/m^2, $\sigma_{xy}^{\infty} = 0$ and $\sigma_{x1}^{\infty} \neq 0$. Take $\beta = 30°$ and $45°$, the normalized Mode I SIF K_{I}/K_0 ($K_0 = \sqrt{\pi l/2}/\sigma_{yy}^{\infty}$) at crack tip A is illustrated in Fig. 4(a) and (b) as a function of the normalized distance l'/l for different remote electric displacement loading D_2^{∞}.

From Fig. 4, an apparent asymptotic nature of K_{I}/K_0 is found irrespective of loading condition. With increasing l'/l, the value of K_{I}/K_0 approaches to 1. Indeed, as could be imagined, the increasing l'/l always results in a decreasing influence of electric loading on Mode I SIF so that the five curves in each figure almost coincide with each other when l'/l is large enough. However, when the crack is located near the interface (e.g. $l'/l < 0.5$), the electric loading disturbs the value of K_{I}/K_0 significantly so that the five curves diverge far from each other. This means that the remote electric loading takes a great effect on the stability of the crack near the interface in piezoelectric bimaterials. Of the great interest is that a transforming distance, namely the neutral electric loading distance (NELD) l'_{NE}, is found from curves of K_{I}/K_0, at which

Table 1
Material constants of the PZT-5H and PZT-5

	C_{11}	C_{12}	C_{13}	C_{33}	C_{44}	
PZT-5H	126	55	53	117	35.3	(GPa)
PZT-5	121	74.5	75.2	111	21.1	
	e_{31}	e_{33}	e_{15}			
PZT-5H	−6.5	23.3	17			(C/m^2)
PZT-5	−5.4	15.8	12.3			
	ε_{11}	ε_{33}				
PZT-5H	151	130				$\times 10^{-10}$ C/V m
PZT-5	81.7	73.46				

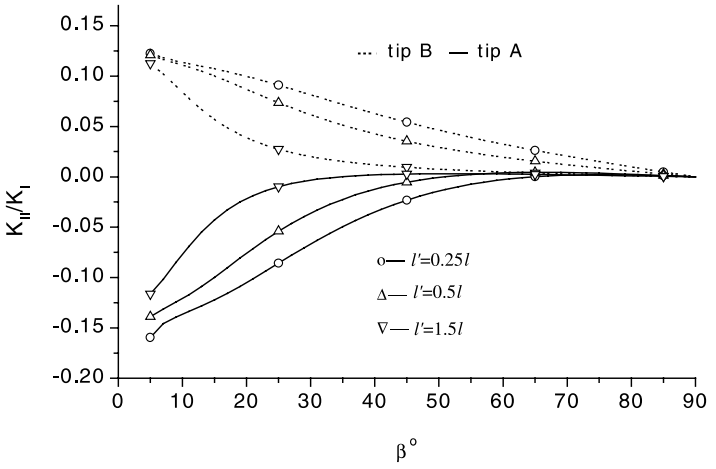

Fig. 3. The ratio of K_{II}/K_I vs. the angle β.

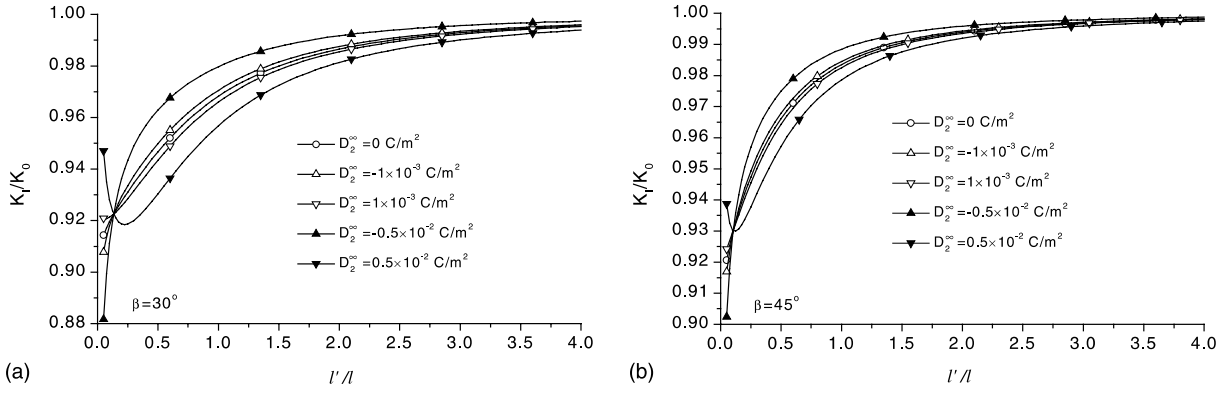

Fig. 4. K_I/K_0 against l'/l: (a) $\beta = 30°$, (b) $\beta = 45°$.

neither positive nor negative electric loading has influence on K_I/K_0. When $l' < l'_{NE}$, the positive electric loading always leads to increasing K_I/K_0, while the negative electric loading decreasing K_I/K_0. However, an opposite influence of electric loading on K_I/K_0 is found when $l' > l'_{NE}$, i.e. the positive electric loading always leads to decreasing K_I/K_0, while the negative electric loading increasing K_I/K_0. The l'_{NE} is equal to about $0.136l$ for $\beta = 30°$ and about $0.107l$ for $\beta = 45°$. It is also seen from the figures that, except $l' = l'_{NE}$, the influence of electric loading on K_I/K_0 always increase along with the increase of its magnitude. In addition, the Fig. 4 shows that all values of K_I/K_0 are smaller than 1, this means that the interface between PZT-5H and PZT-5 has a shielding effect on the crack in PZT-5.

The variation tendency of Mode II SIF K_{II}/K_0 against l'/l at crack tip A is plotted in Fig. 5(a) and (b). Similarly, an apparent asymptotic nature of K_{II}/K_0 is also found from Fig. 5, i.e. the value of K_{II}/K_0 tends to be 0 with increasing l'/l. Moreover, a NELD l'_{NE} is found too, at which neither the positive nor the negative electric loading has influence on K_{II}/K_0. However, the values of the NELD for the Mode II SIF K_{II}/K_0 do not coincide with those shown in Fig. 4 for the Mode I SIF K_I/K_0. They are about $0.26l$ for $\beta = 30°$ and $0.065l$ for $\beta = 45°$. What's more, opposite to the effect of electric loading on K_I/K_0, when $l' < l'_{NE}$, the positive electric loading leads to decreasing K_{II}/K_0, while the negative electric loading

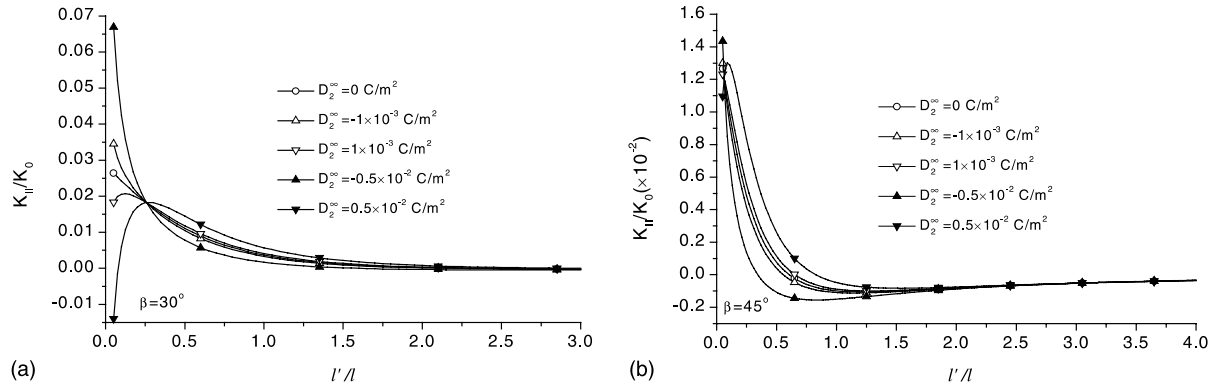

Fig. 5. K_{II}/K_0 against l'/l: (a) $\beta = 30°$, (b) $\beta = 45°$.

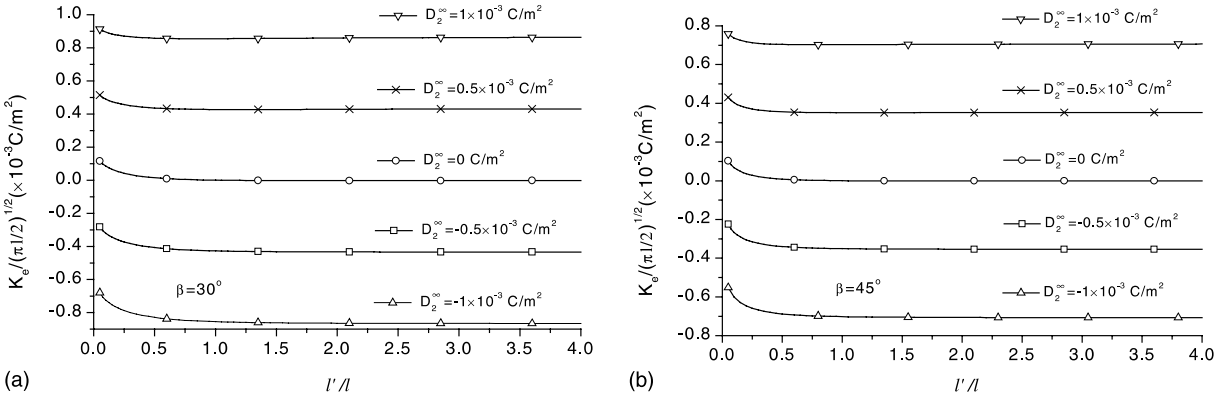

Fig. 6. $K_e/\sqrt{\pi l/2}$ against l'/l: (a) $\beta = 30°$, (b) $\beta = 45°$.

increasing K_{II}/K_0. However when $l' > l'_{\mathrm{NE}}$, the positive electric loading always leads to increasing K_{II}/K_0, while the negative electric loading decreasing K_{II}/K_0.

The EDIFs $K_e/(\pi l/2)^{1/2}$ at tip A against l'/l are plotted in Fig. 6(a) and (b) for $\beta = 30°$ and 45°, respectively. It is found that the positive and negative electric loadings play just opposite roles on EDIF, i.e., the positive electric loading always increases the EDIF, while the negative electric loading always decreases it. It is also seen that, when $l'/l > 1.5$, the influence of l'/l on the EDIF becomes so small that could be neglected completely. But its influence tends to be larger and larger with decreasing l'/l . In addition, whatever the remote electric loading is positive or negative, its increase in magnitude always results in the increasing magnitude of EDIF irrespective of the distance l'/l.

As Park and Sun (1995a,b) pointed out that the MSERR is more suitable to describe the stability and growth of crack in piezoelectric ceramics than the SIF, this parameter should be paid much attention in the present problem. Computed values of the Mode I MSERR $G_{\mathrm{I}}^{\mathrm{M}}$ at crack tip A against l'/l are plotted in Fig. 7(a) and (b) respectively for $\beta = 30°$ and 45°. Here or henceforth, the MSERR is normalized by $G_{\mathrm{I}}^{\mathrm{M}\infty}$ which represents the value of the MSERR for the parallel crack in homogeneous piezoelectric material PZT-5 under pure mechanical loading. It is seen that, similar as found by Park and Sun (1995a,b) for homogeneous piezoelectric solid, the positive electric loading always leads to increasing MSERR and the negative electric loading decreasing it. This indicates that the positive electric loading always promotes the extension

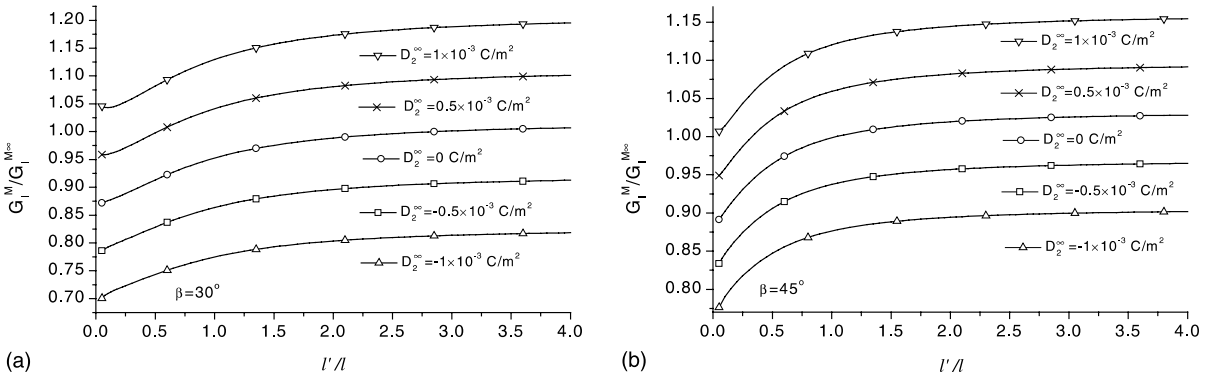

Fig. 7. $G_I^M/G_I^{M\infty}$ against l'/l: (a) $\beta = 30°$, (b) $\beta = 45°$.

of the crack, while the negative electric loading always impedes the extension of the crack. Additionally, in nearly whole range of l'/l, the value of $G_I^M/G_I^{M\infty}$ increases with increasing l'/l and tends to be a constant value when l'/l is large enough. This confirms again that the interface between PZT-5H and PZT-5 actually has a shielding effect on the crack in PZT-5.

Fig. 8(a) and (b) show the results of the normalized J_1/J_0 and J_2/J_0 versus l'/l, where

$$J_0 = \frac{1}{4}\mathbf{K}^{\infty T}\mathbf{H}\mathbf{K}^{\infty} \quad \mathbf{K}^{\infty} = \sqrt{\pi l/2}[\sigma_{xy}^{\infty}; \sigma_{yy}^{\infty}; 0; D_2^{\infty}] \tag{42}$$

It can be found that the J_1-integral vanishes as predicted by Eq. (41), this indicates that the path-independent property of the J_1-integral found in non-piezoelectric bimaterials (Zhao and Chen, 1997) is still valid in piezoelectric bimaterials. However, due to the effect induced from the interface, the J_2-integral does not vanish, and generally speaking, a large influence of the interface on J_2-integral occurs when the distance l'/l is decreased.

Let $l'/l = 0.25$ and 1.0, the values of MSERR against the orientation angle β are illustrated in Fig. 9(a) and (b), respectively. It is found that when $\beta = 90°$, i.e. the crack is perpendicular to the interface, whatever the positive or the negative electric loading takes no effect on the MSERR. Except this special location of the crack, the positive electric loading always increases the MSERR, while the negative electric loading always decreases it. This confirms for another time that, in most range of β, the positive electric loading

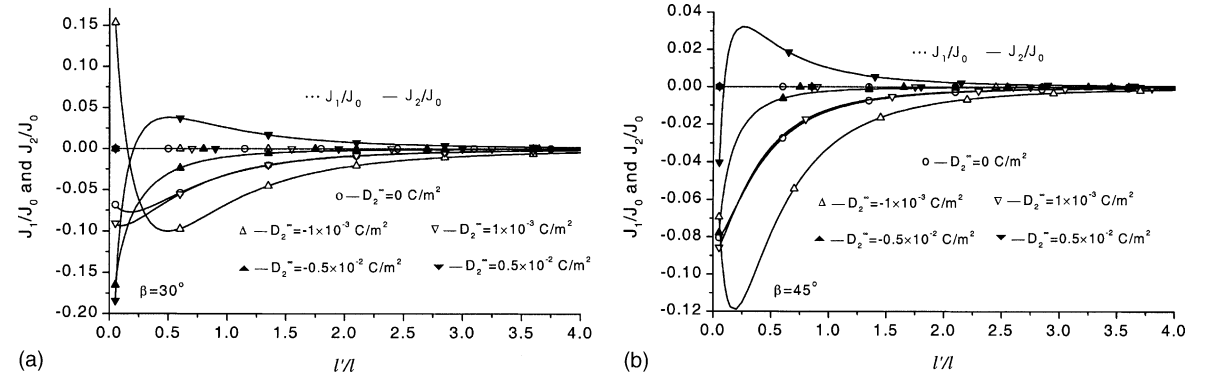

Fig. 8. J_1/J_0 and J_2/J_0 against l'/l: (a) $\beta = 30°$, (b) $\beta = 45°$.

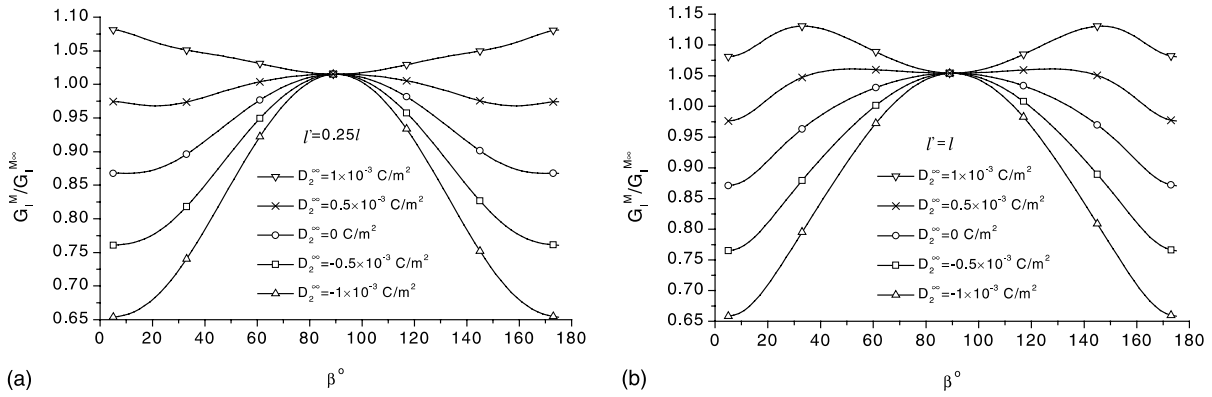

Fig. 9. $G_{\mathrm{I}}^{\mathrm{M}}/G_{\mathrm{I}}^{\mathrm{M}\infty}$ against the angle β: (a) $l' = 0.25l$, (b) $l' = l$.

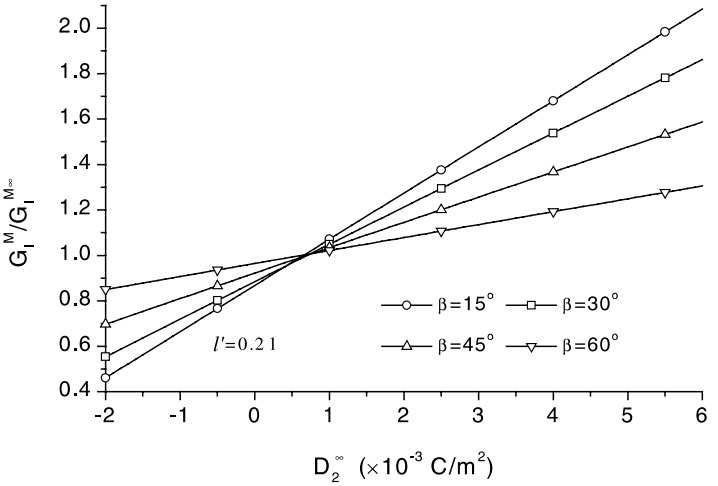

Fig. 10. $G_{\mathrm{I}}^{\mathrm{M}}/G_{\mathrm{I}}^{\mathrm{M}\infty}$ against the electric displacement D_2^{∞}.

really promotes the extension of the crack, while the negative electric loading impedes it. It is also found that, with the increasing diversion of β from 90°, the disturbance of the electric loading on the MSERR tends to be strong, so that five curves diverge farther and farther from each other.

Fig. 10 shows the variation of the MSERR at crack tip A for several values of β as a function of the remote electric loading D_2^{∞}. It is found that the variation tendencies of the MSERR against the electric loading are linear and the line slope increases with decreasing β. This fully proves that the influence of the electric loading on the MSERR tends to increase when the crack approaches to the interface.

7. Conclusions

From above investigations and discussions, the following conclusions can be obtained:

(1) The proposed dislocation method is actually effective for solving the near interface crack problem in piezoelectric bimaterials.

(2) The remote electric loading takes a great effect on the stability of the near interface crack in piezoelectric bimaterials. Moreover, its influence tends to increase when the crack approaches to the interface.
(3) In the combination of PZT-5H/PZT-5, the interface between PZT-5H and PZT-5 always has a shielding effect on the crack in PZT-5.
(4) The positive and negative electric loadings play opposite roles on the EDIF, i.e., the positive electric loading always increases the EDIF, while the negative electric loading always decreases it. Moreover, whatever the remote electric loading is positive or negative, its increasing value always leads to the increase of EDIF in magnitude.
(5) Generally speaking, the positive electric loading leads to increasing the MSERR and the negative electric loading decreasing it. This indicates that the positive electric loading generally promotes the extension of the crack, while the negative electric loading generally impedes the extension of the crack.
(6) The MSERR changes linearly with the variation of the remote electric displacement loading. Moreover, the MSERR tends to be more sensitive to the modification of electric displacement loading with the decreasing orientation angle of the crack. It can be predicted that, when the poling direction is perpendicular to the interface, the remote electric displacement loading will bring the largest influence on the MSERR for a parallel near interface crack, while bring a least influence on the MSERR for a perpendicular one.
(7) The J_1-integral is still path independent in piezoelectric bimaterials though both the stress and electric fields are taken into account.

Acknowledgement

This work was supported by the Hong Kong Polytechnic University Post-doctoral Project (no. G-YW53).

References

Barnett, D.M., Lothe, J., 1975. Dislocations and line changes in anisotropic piezoelectric insulators. Phys. Status Solidi. B 67, 105–111.
Budiansky, B., Rice, J.R., 1973. Conservation laws and energy release rate. ASME J. Appl. Mech. 40, 201–203.
Deeg, W.F., 1980. The analysis of dislocation, crack, and inclusion problems in piezoelectric solids. Ph.D. thesis, Stanford University.
Erdogan, F., 1978. Mixed boundary-value problem in mechanics. In: Nemat-Nasser, S. (Ed.), Mechanics Today, 4. Pergamon Press, pp. 1–86.
Fulton, C.C., Gao, H., 1997. Electrical nonlinearity in fracture of piezoelectric ceramics. Appl. Mech. Rev. 50, S56–S63.
Gao, H., Zhang, T.Y., Tong, P., 1997. Local and global energy rates for an electrically yielded crack in piezoelectric ceramics. Ferroelectrics 166, 11–13.
Han, J.J., Chen, Y.H., 1999. Multiple parallel cracks interaction problem in piezoelectric ceramics. Int.J. Solids Struct. 36, 3375–3390.
He, M.Y., Hutchinson, J.W., 1989. Kinking of a crack out of an interface. ASME J. Appl. Mech. 56, 270–278.
Herrmann, A.G., Herrmann, G., 1981. A path-independent integral and the approximate analysis. ASME J. Appl. Mech. 48, 525–528.
Lu, H., Lardner, T.J., 1992. Mechanics of subinterface cracks in layered material. Int. J. Solids Struct. 29, 669–688.
McMeeking, R.M., 1990. A J-integral for the analysis of electrically induced mechanical stress at cracks in elastic dielectrics. Int. J. Eng. Sci. 28, 607–613.
Miller, G.R., 1989. Analysis of cracks near interfaces between dissimilar anisotropic materials. Int. J. Eng. Sci. 27, 667–678.
Pak, Y.E., 1990. Crack extension force in a piezoelectric material. ASME J. Appl. Mech. 57, 647–653.
Pak, Y.E., 1992. Linear electro-elastic fracture mechanics of piezoelectric materials. Int. J. Fract. 54, 79–100.
Park, S.B., Sun, C.T., 1995a. Fracture criteria for piezoelectric ceramics. J. Am. Ceram. Soc. 78, 1475–1480.
Park, S.B., Sun, C.T., 1995b. Effect of electric fields on fracture of piezoelectric ceramics. Int. J. Fract. 70, 203–216.
Qin, Q.H., Mai, Y.W., 2000. Crack branch in piezoelectric bimaterial system. Int. J. Eng. Sci. 38, 673–693.
Soh, A.K., Fang, D.N., Lee, K.L., 2000. Analysis of a bi-piezoelectric ceramic layer with an interfacial crack subjected to anti-plane shear and in-plane electric loading. Eur. J. Mech. A/Solids 19, 961–977.

Sosa, H., 1991. Plane problems in piezoelectric media with defects. Int. J. Solids Struct. 28, 491–505.
Sosa, H., 1992. On the fracture mechanics of piezoelectric solids. Int. J. Solids Struct. 29, 2613–2622.
Sosa, H., Pak, Y.E., 1990. Three-dimensional eigenfunction analysis of a crack in a piezoelectric material. Int. J. Solids Struct. 26, 1–15.
Suo, Z., 1990. Singularities, interfaces and cracks in dissimilar anisotropic media. Proc. R. Soc. Lond. A 427, 331–358.
Suo, Z., Hutchinson, J.W., 1989. Steady-state cracking in brittle subinterface beneath adherent films. Int. J. Solids Struct. 25, 1337–1353.
Suo, Z., Kuo, C.M., Barnett, D.M., Willis, J.R., 1992. Fracture mechanics for piezoelectric ceramics. J. Mech. Phys. Solids 40, 739–765.
Zhao, L.G., Chen, Y.H., 1997. Further investigation of subinterface cracks. Arch. Appl. Mech. 67, 393–406.